

# Turbulent Pipe Flow Near-Wall Statistics

Tommaso Fiorini, Gabriele Bellani, Ramis Örlü, Antonio Segalini, P. Henrik Alfredsson and Alessandro Talamelli

**Abstract** Results from the first experimental campaign in the Long Pipe facility of the CICLoPE laboratory are reported. Single hot-wire profile measurements are presented, taken from the wall up to one third of the pipe radius, with the friction Reynolds number  $Re_\tau$  ranging from  $6.5 \times 10^3$  up to  $3.8 \times 10^4$ . Measurements of the pressure drop along the pipe are presented together with an estimation of its uncertainty. Mean and variance of the streamwise velocity fluctuations are examined and compared with the findings from other facilities. The amplitude of the inner-scaled near-wall peak of the variance, after being corrected for spatial resolution effects, shows an increasing trend with Reynolds number, in accordance with low Reynolds number experiments and simulations.

## 1 Introduction

Turbulent pipe flow is one of the canonical wall flows, and it has been the object of a multitude of studies over the years. Direct numerical simulations (DNS) and experiments have progressively led to an improved understanding of wall turbulence, but despite being intensively studied, many issues remain unresolved, such as the *Re*-scaling of the variance profile (see [1–3]). Laboratory experiments continue to play an essential role in the understanding of the physics of wall-bounded turbulence, since DNS are still limited to low *Re*. The CICLoPE Long Pipe facility [4] aims at shedding light on some of the open questions of wall turbulence. The facility is unique in its kind, due to its very large dimensions, high *Re* can for the first time be reached while still maintaining a sufficient spatial resolution to resolve all the scales of turbulent motion with conventional hot-wire sensors. Spatial filtering is a great challenge in experiments [5], and has been masking the true nature of turbulence at high *Re*. Beside the resolution, the facility's high degree of manufacturing tolerances and

---

T. Fiorini · G. Bellani · A. Talamelli (✉)  
DIN, Università di Bologna, 47100 Forlì, Italy  
e-mail: alessandro.talamelli@unibo.it

R. Örlü · A. Segalini · P.H. Alfredsson  
Linné FLOW Centre, KTH Mechanics, 10044 Stockholm, Sweden

© Springer International Publishing AG 2017  
R. Örlü et al. (eds.), *Progress in Turbulence VII*, Springer Proceedings  
in Physics 196, DOI 10.1007/978-3-319-57934-4\_13

flow stability provide the possibility to carry out accurate and resolved experiments at high  $Re$ , in a way that has so far not been possible in any other wall-turbulence facility.

## 2 Experimental Setup

The Long Pipe facility in the CICLoPE laboratory is a closed-loop wind tunnel, where at the end of the test section, a 111 m long carbon-fiber pipe, a fully developed turbulent flow condition is reached. The pipe has an inner diameter of  $901 \pm 0.1$  mm, resulting in a length-to-diameter ratio of  $L/D \approx 123$ . The dimension of the facility is the result of the sizing process detailed in [4]. The wind tunnel is also equipped with flow conditioning elements to ensure a good and stable flow quality; these include a heat exchanger, a honeycomb, 5 screens, a settling chamber, and a convergent with contraction ratio of 4; each of the six corners of the loop is also equipped with turning vanes. The wind tunnel is driven by two-stage axial fans for a total power of 480 kW, however for the present measurements only one fan was used and the other was free running. For technical details about the final design of the facility and its elements, the reader is referred to [6]. In Fig. 1 an overview of the facility with its principal elements is shown. Hot-wire anemometry measurements are performed close to the end of the test section at  $L/D = 122$ , as a part of the same experimental campaign described in [4], but here a new hot-wire data-set with a shorter sensor is shown. The data presented here are acquired with a custom-made boundary-layer type probe, with a  $1.2 \mu\text{m}$  diameter platinum wire soldered on stainless steel prongs; the wire length is 0.25 mm in order to keep a wire aspect ratio of  $l/d \approx 200$ . The hot-wire is operated in constant-temperature mode via a Dantec Streamline system. The sampling frequency is set to 60 kHz with an analog low-pass filter at 30 kHz for all cases. Velocity calibration was performed ex situ in a DANTEC Streamline 90H02 external calibrator jet. The hot-wire probe is mounted on a traversing system that consists of a hollow carbon-fiber airfoil that slides through the pipe wall (see Fig. 2) and spans from the wall up to  $y/R \approx 0.3$ ; where  $y$  is the wall-normal distance and  $R$  is the pipe radius. The probe is traversed via a stepper motor with a  $5 \mu\text{m}$  resolution step, while the relative position is obtained using a Renishaw Tonic T100x

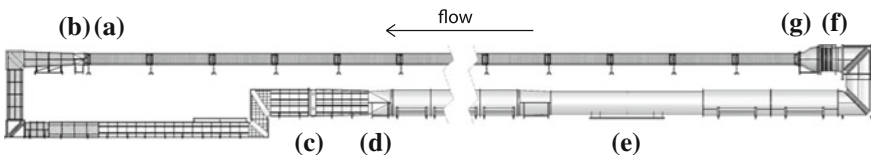


**Fig. 1** Overview of the Long Pipe flow loop. **a** Measuring station. **b** Round to rectangular shape converter. **c** Heat exchanger. **d** Rectangular to round shape converter. **e** Axial fans. **f** Flow conditioning unit (honeycomb, screens). **g** Convergent with contraction ratio 4

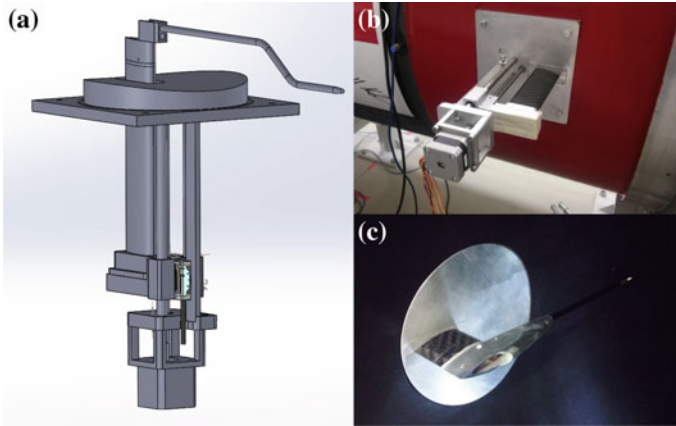


**Fig. 2** The traversing device used for the hot-wire measurements, described in Sect. 2. **a** CAD drawing of the device. **b** Traversing as seen from outside the pipe, including the stepper motor and optical encoder. **c** Traversing as seen from inside the pipe, showing the probe holder and sting assembly

optical linear encoder with a  $0.5 \mu\text{m}$  resolution. The mean centreline velocity is measured with a Prandtl tube connected to a MKS Baratron 120AD differential pressure transducer with a 1333 Pa range. The ambient pressure and temperature inside the test chamber are acquired with a MKS Baratron 120A absolute pressure transducer and a PT100 platinum thermoresistor, respectively. The pressure along the pipe is acquired through 16 static pressure taps, with a hole diameter of 1 mm, connected to a digital pressure scanner Initium with 2500 Pa range.

### 3 Pressure Drop Measurement

The pressure taps used to determine the pressure drop inside the pipe are located from the hot-wire measuring station up to 70 m upstream, with a 5 m spacing between each of them. To obtain the pressure gradient  $dp/dx$  and therefore the wall friction  $\tau_w$ , a least-square fitting is performed. In order to determine the region and number of pressure taps to use, different linear fits of the data have been made starting from the test section and moving upstream using an increasing number of points for a wide range of friction Reynolds number  $Re_\tau$ , where  $Re_\tau = u_\tau R/\nu$ , with  $u_\tau$  denoting the friction velocity and  $\nu$  the kinematic viscosity of the fluid. To evaluate the quality of those fits, their uncertainty can be computed, as shown in Fig. 3a. The more measurement points are used, the less the fit is influenced by bias errors introduced by single pressure taps; on the other hand, a local measure at the hot-wire station is desired, and an overall lower uncertainty of the fit does not necessarily mean that

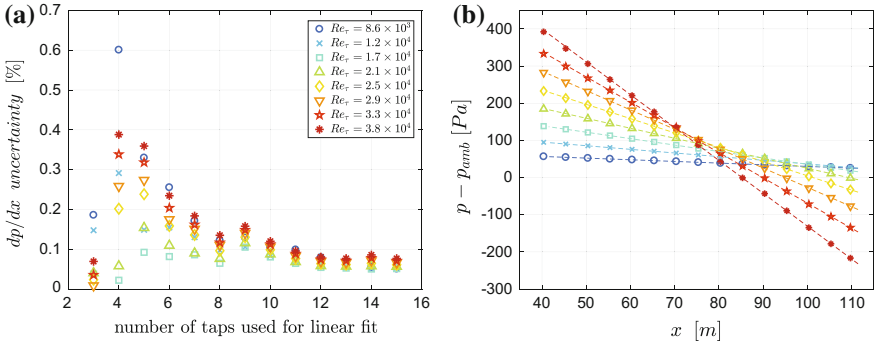


**Fig. 3** **a** Uncertainty on the linear fit used to determine  $dp/dx$ , as a function of the number of pressure taps used for the fit. **b** Difference between the static pressure measured along the pipe and the ambient pressure, where  $x$  indicates the axial distance from the start of the pipe. *Dashed lines* indicate the linear fits obtained by using the last 6 points

the  $dp/dx$  at the hot-wire station is measured more accurately. Only relatively small benefits are visible by adding more data points beyond the 6th–7th tap. It was thus decided to compute the pressure gradient using the last 6 pressure taps corresponding to the last 30 m of the pipe, to avoid any residual flow development effect. Static pressure data points and corresponding linear fits calculated in this way are shown in Fig. 3b for a range of Reynolds number.

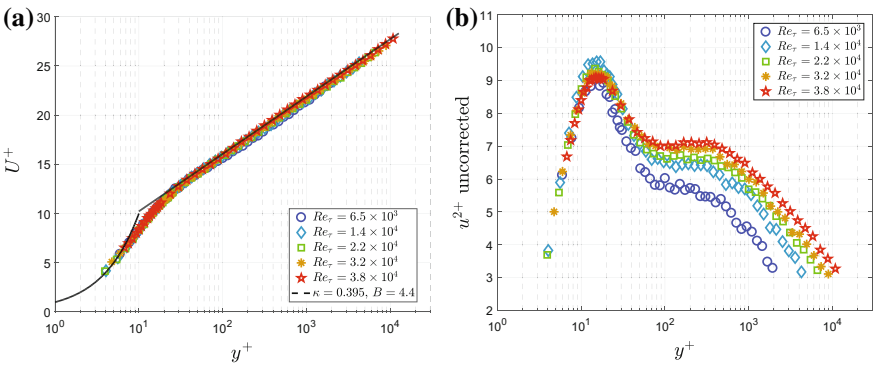


**Fig. 4** **a** Inner-scaled mean velocity profile. *Solid black line* shows a logarithmic law with coefficients given in the legend. **b** Inner-scaled streamwise velocity variance without any correction applied

### 4 Near-Wall Statistics

Single-wire velocity profiles were acquired with the traversing system described in Sect. 2, the pressure drop was acquired and averaged for the duration of the profile acquisition. A calibration was performed before and after each profile to check for sensor drift. The mean velocity normalized with the friction velocity,  $U^+$ , is shown in Fig. 4a. The absolute wall position was retrieved by fitting the data points for  $U^+ < 10$  using an analytical expression for the law of the wall [7]. The friction velocity was obtained directly from the pressure drop as outlined in Sect. 3. Data collapse is satisfying with a slight deviation on the dataset at the lowest  $Re$ , i.e.  $Re_\tau = 6.5 \times 10^3$ , which might be related to insufficient calibration data points for the lowest velocity range, or to the increased uncertainty in the pressure drop determination. The normalized mean velocity profiles are shown together with the linear relationship of the viscous sublayer and a reference logarithmic law with coefficients  $\kappa = 0.395$  and  $B = 4.40$ . It should be noted that an accurate analysis of the mean velocity logarithmic region, its limits and the value of the coefficients has yet to be performed, and the value of the coefficients given here are just for reference. The coefficients of the log law also appear to differ slightly from what is measured in [8], where different hot-wire data-sets from the same experimental campaign are presented. The measured streamwise velocity variance normalized with the friction velocity,  $u^{2+}$ , is shown in Fig. 4b; data was then corrected using the semi-empirical expression reported in [9] and the corrected variance is shown in Fig. 5a. The corrected  $u^{2+}$ , shows a clear trend in the magnitude of the near-wall peak with increasing Reynolds number, particularly visible at lower  $Re_\tau$ , as such confirming the findings from channel and boundary layers [5, 10], while differing from observations from the Princeton University/ONR Superpipe facility [11, 12]. The  $Re$ -trend of

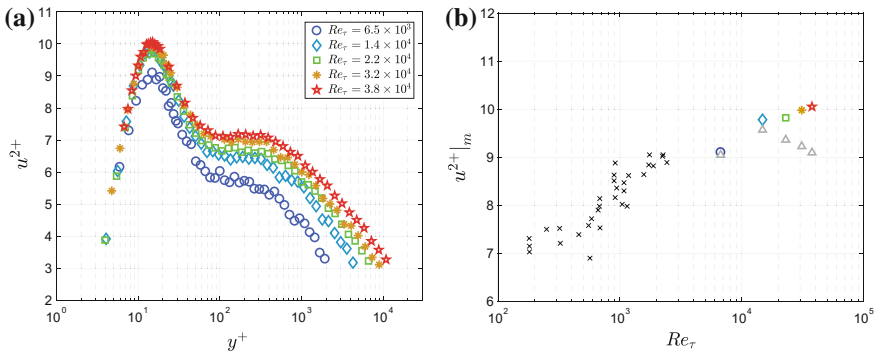


**Fig. 5** **a** Inner-scaled streamwise velocity variance after being corrected with the scheme proposed in [9] **b** Amplitude of the variance near-wall peak  $u^{2+}|_m$ , as a function of the friction Reynolds number.  $\times$  symbols represent data reported in [14],  $\Delta$  symbols are the data from present measurements whereas the *coloured* symbols show the same data corrected for spatial averaging using [9]

the amplitude of the near-wall peak is given in Fig. 5b together with some results measured in the KTH pipe facility [13, 14]. As far as the ‘second peak’ observed in other pipe flow experiments [11, 12, 15, 16] and predicted in [17] is concerned, the present results cannot confirm its presence, as no clear peak is visible up until the highest Reynolds number investigated here ( $Re_\tau = 3.8 \times 10^4$ ). Nevertheless, it should be noted that in the Superpipe measurements, at these Reynolds number, such a peak has only started to appear and is still quite ‘subtle’ in appearance.

**Acknowledgements** Financially supported through the European High-Performance Infrastructures in Turbulence (EuHIT) within the Reynolds stress tensor scaling in turbulent pipe flow (Re-Scale) project.

## References

1. I. Marusic, B.J. McKeon, P.A. Monkewitz, H.M. Nagib, A.J. Smits, K.R. Sreenivasan, Wall-bounded turbulent flows at high Reynolds number: recent advance and key issues. *Phys. Fluids* **22**, 065103 (2010)
2. J. Kim, Progress in pipe and channel flow turbulence 1961–2011. *J. Turbul.* **13**, N45 (2012)
3. A.J. Smits, B.J. McKeon, I. Marusic, High-Reynolds number wall turbulence. *Annu. Rev. Fluid Mech.* **43**, 353–375 (2011)
4. A. Talamelli, F. Persiani, J.H.M. Fransson, P.H. Alfredsson, A.V. Johansson, M. Nagib, H. Rüedi, J.-D. Sreenivasan, P.A. Monkewitz, CICLOPE—a response to the need for high Reynolds number experiments. *Fluid Dyn. Res.* **41**, 021407 (2009)
5. N. Hutchins, T.B. Nickels, I. Marusic, M.S. Chong, Hot-wire spatial resolution issues in wall-bounded turbulence. *J. Fluid Mech.* **635**, 103–136 (2009)
6. G. Bellani, A. Talamelli, The final design of the long pipe in CICLOPE, in *Springer Proceedings in Physics, Progress in Turbulence VI*, Springer, pp. 205–209 (2016)
7. K.A. Chauhan, P.A. Monkewitz, H.M. Nagib, Criteria for assessing experiments in zero pressure gradient boundary layers. *Fluid Dyn. Res.* **41**, 021404 (2009)
8. R. Örlü, T. Fiorini, G. Bellani, A. Segalini, P.H. Alfredsson, A. Talamelli, Reynolds stress scaling in pipe flow turbulence—first results from CICLOPE. *Phil. Trans. R. Soc. A* **375**, 20160187 (2017)
9. A.J. Smits, J. Monty, M. Hultmark, S.C.C. Bailey, N. Hutchins, I. Marusic, Spatial resolution correction for wall-bounded turbulence measurements. *J. Fluid Mech.* **676**, 41–53 (2011)
10. P.H. Alfredsson, R. Örlü, A. Segalini, A new formulation for the streamwise turbulence intensity distribution in wall-bounded turbulent flows. *Eur. J. Mech. B/Fluids* **36**, 167–175 (2012)
11. M. Hultmark, S.C.C. Bailey, A.J. Smits, Scaling of near-wall turbulence in pipe flow. *J. Fluid Mech.* **649**, 103–113 (2010)
12. M. Hultmark, M. Vallikivi, S.C.C. Bailey, A.J. Smits, Turbulent pipe flow at extreme Reynolds numbers. *Phys. Rev. Lett.* **779**, 371–389 (2012)
13. M. Ferro, Experimental study on turbulent pipe flow. M.Sc. Thesis, KTH Mechanics, Royal Institute of Technology, Stockholm (2012)
14. R. Örlü, P.H. Alfredsson, Comment on the scaling of the near-wall streamwise variance peak in turbulent pipe flows. *Exp. Fluids* **54**, 1431 (2013)
15. J.F. Morrison, B.J. McKeon, W. Jiang, A.J. Smits, Scaling of the streamwise velocity component in turbulent pipe flow. *J. Fluid Mech.* **508**, 99–131 (2004)
16. M. Vallikivi, M. Hultmark, S.C.C. Bailey, A.J. Smits, Turbulence measurements in pipe flow using a nano-scale thermal anemometry probe. *Exp. Fluids* **51**, 1521–1527 (2011)
17. P.H. Alfredsson, A. Segalini, R. Örlü, A new scaling for the streamwise turbulence intensity in wall-bounded turbulent flows and what it tells us about the “outer” peak. *Phys. Fluids* **23**, 041702 (2011)